

#### Facultad de Ingeniería

#### Maestría en Hidrología con mención en Ecohidrología

How do hydrometeorological storm event variables influence the concentrationdischarge hysteresis during events in a Páramo ecosystem?

> Trabajo de titulación previo a la obtención del título de Magíster en Hidrología con mención en Ecohidrología

#### Autor:

Ing. Pablo Gabriel Peña Saltos

CI: 0301546024

Correo electrónico: pablogabrielpenasaltos@gmail.com

#### Director:

Ing. Patricio Javier Crespo Sánchez, Ph.D.

CI: 0102572773

Cuenca, Ecuador

13-julio-2022



#### Resumen:

Los factores hidrometeorológicos son identificados como los principales factores desencadenantes de la variabilidad química de la corriente fluvial. La identificación adecuada de estos factores proporcionará una mirada profunda al funcionamiento de las cuencas. En este contexto, el estudio de las relaciones concentración-caudal (C-Q) representa una forma óptima de evaluar los mecanismos de movilización de solutos en el río. A través del uso de un conjunto de datos de alta frecuencia y un análisis de correlación, entre las variables de eventos hidrometeorológicos y un índice de histéresis, el siguiente estudio identificó los principales controles hidrometeorológicos sobre la respuesta histérica en una cuenca tropical de alta montaña. Los resultados nos permiten explorar los principales grupos de respuestas de histéresis de los solutos estudiados (Al, Cu, DOC, TNb, Ba, Ca, Mg, Na, Sr, K, Si, Rb) infiriendo vías de movilización y estado químico del evento en términos de enriquecimiento o agotamiento bajo diferentes condiciones de humedad.

Palabras claves: Histéresis. Curvas concentración-caudal. Trópicos. Páramo



#### **Abstract:**

Hydrometeorological factors are identified as the main triggering factors of the stream chemistry variability. Proper identification of these factors will provide a deep look into catchments functioning. In this context, studying concentration-discharge (C-Q) relationships represent an optimal manner to assess the solutes delivery mechanisms in the river. Through the use of a high-frequency data set and a correlation analysis, between hydrometeorological storm event variables and a hysteresis index, the following study identified main hydrometeorological controls on the hysteric response in a high-mountain tropical catchment. The results let us explore the main groups of hysteresis responses of the studied solutes (AI, Cu, DOC, TNb, Ba, Ca, Mg, Na, Sr, K, Si, Rb) inferring mobilization pathways and event chemical status in terms of enrichment or depletion under different moisture conditions.

**Keywords:** Hysteresis. Concentration-discharge loops. Tropics. Páramo



#### Índice del Trabajo

1. Int	roduction	9
2. Ma	iterials & Methods	11
2.1	Study Area	11
2.2	Data Collection	13
2.3	Storm Analysis	14
2.4	Hysteresis Loop Characterization	16
2.5	Analysis of the Hysteresis Indicators Variability Controls	18
3. Re	sults	19
3.1	Storm Analysis	19
3.2	Hysteresis Loop Characterization	21
3.3	Analysis of the Hysteresis Indicators Variability Controls	23
4. Dis	scussion	32
4.1	Hysteresis Loop Characterization	32
4.2	Analysis of the Hysteresis Indicators Variability Controls	34
5. Co	nclusions	37
6. Re	ferences	37



#### Índice de Figuras

Figure 1. Zhurucay experimental catchment	12
Figure 2 Hysteresis loop types occurrancy percentage	22
Figure 3 Two hydrological events with different hysteresis responses	23
Figure 4 Chemical status categorization	26
Figure 5 Visual relationships between range of discharge (Range Q.) and the cal	culated
hysteresis index (HI)	29
Figure 6 Visual relationships between range of discharge (Range Q.) and the hys	steresis
loop area	31



#### Índice de Tablas

Table 1 Computed storm variables.	15
Table 2 Summary statistics of the 85 events identified.	19
Table 3 Summary of the random forest and correlation analysis between the event	
variables (precipitation, concentration, discharge) and the calculated hysteresis index	
(HI)	27
Table 4 Summary of the random forest and correlation analysis between the event	
variables (precipitation, concentration, discharge) and the calculated loop area	28



#### UCU Clávsula de licencia y autorización para publicación en el Repositorio Institucional

Yo, Pablo Gabriel Peña Saltos, en calidad de autor y titular de los derechos morales y patrimoniales del trabajo de titulación "How do hydrometeorological storm event variables influence the concentration-discharge hysteresis during events in a Páramo ecosystem?", de conformidad con el Art. 114 del CÓDIGO ORGÁNICO DE LA ECONOMÍA SOCIAL DE LOS CONOCIMIENTOS, CREATIVIDAD E INNOVACIÓN reconozco a favor de la Universidad de Cuenca una licencia gratuita, intransferible y no exclusiva para el uso no comercial de la obra, con fines estrictamente académicos.

Asimismo, autorizo a la Universidad de Cuenca para que realice la publicación de este trabajo de titulación en el repositorio institucional, de conformidad a lo dispuesto en el Art. 144 de la Ley Orgánica de Educación Superior.

Cuenca, 12 de julio de 2022

Pablo Gabriel Peña Saltos

C.I. 0301546024







#### Cláusula de Propiedad Intelectual

Yo, Pablo Gabriel Peña Saltos, autor del trabajo de titulación "How do hydrometeorological storm event variables influence the concentration-discharge hysteresis during events in a Páramo ecosystem?", certifico que todas las ideas, opiniones y contenidos expuestos en la presente investigación son de exclusiva responsabilidad de su autor.

Cuenca, 12 de julio de 2022

Pablo Gabriel Peña Saltos

C.I. 0301546024



#### 1. Introduction

Streams chemistry can vary strongly in time and space due to intrinsic catchment characteristics (e.g., soil properties, climate, anthropogenic activities, etc.). The hydrological catchment behavior is identified as one of the main triggering factors of the solute dynamics (Butturini et al., 2008; McClain et al., 2003). An interesting way to understand the solute dynamic behavior is studying individual hydrological events that constitute mobilization of particles from the catchment compartments (vegetation, soils, springs, etc.) to the streams (Biron et al., 1999). This solute delivery mechanism can be described using concentration-discharge relationships (Walling & E., 1974; Williams, 1989). These relationships create a hysteric behavior in which same discharge values could represent different or similar solute concentration values on the rising and falling limb of the hydrological event, depending on the ecohydrological characteristics of the catchment, during and / or before the hydrological event (O'Kane, 2005; Phillips, 2003). Categorization of this hysteric behavior have been used to identify controls on stream solute fluxes for a long time, given that they can expose hydrochemical processes besides the origin and fate of delivered materials, providing a deep look into the catchment functioning (Chanat et al., 2002; C. Evans & Davies, 1998; Jiang et al., 2010; Murphy et al., 2014).

With the objective of categorize hysteresis loops, qualitatively (based on the hysteresis shape and direction) (Williams, 1989), and quantitatively (based on hysteresis indices: HI), different approaches are used (Butturini et al., 2008; Langlois et al., 2005; Lawler et al., 2006; Lloyd et al., 2016b; Zuecco et al., 2016). The most of these HI are based on the quantification of shape, extent and direction of the hysteresis loops and are computed using ratio relationships between solute concentration values on the rising and falling limb of the hydrograph. In this context and to avoid presumably under estimations of HI when complex loops are being analyzed, it has been developed an index which use the difference between the solute concentration values on the rising and falling limbs of the normalized storms, instead of ratio relationships (Lloyd et al., 2016b). Streamflow and

stream chemistry data, at high frequency resolutions, is required at the studied catchment outlet in order to compute Lloyd Index (C. Evans & Davies, 1998; Lloyd et al., 2016b). To record this high resolution data, in situ water quality sensors (e.g.: based on spectrometry techniques) could be used. They produce detailed descriptions of solute chemical behaviors (Jones et al., 2011; Kirchner et al., 2004; Pesántez et al., 2021), considering information that would usually be ignored at higher resolutions (Bowes et al., 2009, 2015; Kirchner et al., 2004; Madrid & Zayas, 2007; Robson et al., 1991).

In conjunction with the qualitative and quantitative hysteresis, the analysis of solute chemical status at C-Q relationships, allows us to deeply explore certain ecohydrological processes. This knowledge leads to a better understanding of the processes that govern the early or late solute source depletion and its seasonal changes (Zuecco et al., 2016). The states of the events based on chemical status at C-Q relationships can be categorized in: chemostasis, mobilization and dilution (Basu et al., 2011; Chanat et al., 2002; Godsey et al., 2009; Herndon et al., 2015; Maher, 2011). When the solute delivery depends on some physical factors rather than discharge variation, a chemostatic behavior is pointed out (Godsey et al., 2009). When discharge becomes an important factor for the solute delivery, the characteristically chemical status may be mobilization or dilution of solutes. The first one describes the increasing solute concentrations with discharge and the second one, the opposite case, decreasing solute concentrations with increasing discharge (Chanat et al., 2002; Maher, 2011) representing different ecohydrological states also in the catchment.

Against this background, recent studies have identified a strong influence of climate, catchment size, lithology, anthropogenic activities and hydrometeorological behaviors on the stream chemistry variability (Creed et al., 2015; Godsey et al., 2019; Hale & Godsey, 2019; Moatar et al., 2017; Stallard & Murphy, 2013). It has previously been observed that the variation of mean solute concentrations can be described as a function of mean runoff, when solutes originated from bedrock weathering process are being analyzed (Godsey et al., 2019). Weather and climate cause changes in precipitation patterns, modifying the solute rainfall inputs to catchments (Godsey et al., 2019; Hornberger et al., 2001; Tardy

et al., 2004). Inner soil characteristics influence shifts among dominant flowpaths, such as groundwater and shallow paths, producing water table elevation variations. All these factors directly influence the C-Q catchment response (Daley et al., 2009; Ibarra et al., 2016; Winnick et al., 2017). Identification of hysteresis controls drives to reveal valuable information about catchment functioning. These include biogeochemical cycles, runoff generation mechanisms, effects of antecedent environmental moisture conditions on chemical stream variability and connectivity between solute sources and streams (Murphy et al., 2014; Shanley et al., 2015; Spence, 2010; Wymore et al., 2017).

Thanks to the intensive hydrometeorological and chemical monitoring campaign and instrumentation developed at the Zhurucay Ecohydrological Observatory (ZEO), we are able to manage 5min-frequency hydrological and water quality data (from an optical sensor) from March 2018 to March 2019. In this sense, the main objective of the following study is to identify the most important hydrometeorological controls (precipitation, concentration, discharge) of hysteresis metrics (HI, loop area) variability of a considerable range of representative solutes (AI, Cu, DOC, TNb, Ba, Ca, Mg, Na, Sr, K, Si, Rb), during storm events in a small high-mountain tropical catchment. The concluding results of this study will let us set a baseline of the current hysteresis response to hydrometeorological factors at a high Andean tropical catchment, driving us to a quantitative guide of future disturbances (under anthropogenic and climate changes pressures), which represents a necessary topic in the implementation of properly management and conservation guidelines for the water resource.

#### 2. Materials & Methods

#### 2.1 Study Area

The study catchment is located within the Zhurucay Ecohydrological Observatory (ZEO), this pristine tropical headwater catchment (3.28 km2) that has served as an experimental site since 2010. It is located in the southern region of the Andean mountain range in

Ecuador (*Figure 1.* Zhurucay experimental catchment, highlighting a) the distribution of the streams, the two main types of soil (Histosols, Andosols), besides the position of the monitoring points of precipitation and discharge/solute chemistry at the microcatchment outlet, and b) its location on the Ecuadorian geography.). Generally, the climate is affected by both Atlantic and Pacific regimes (Crespo et al., 2011), which is the main reason for the low seasonality of rainfall (Padrón et al., 2015). From March 2018 to March 2019, we measured and computed mean annual precipitation, it is 1245 mm and the mean annual discharge at the catchment outlet is 582 mm year<sup>-1</sup>.

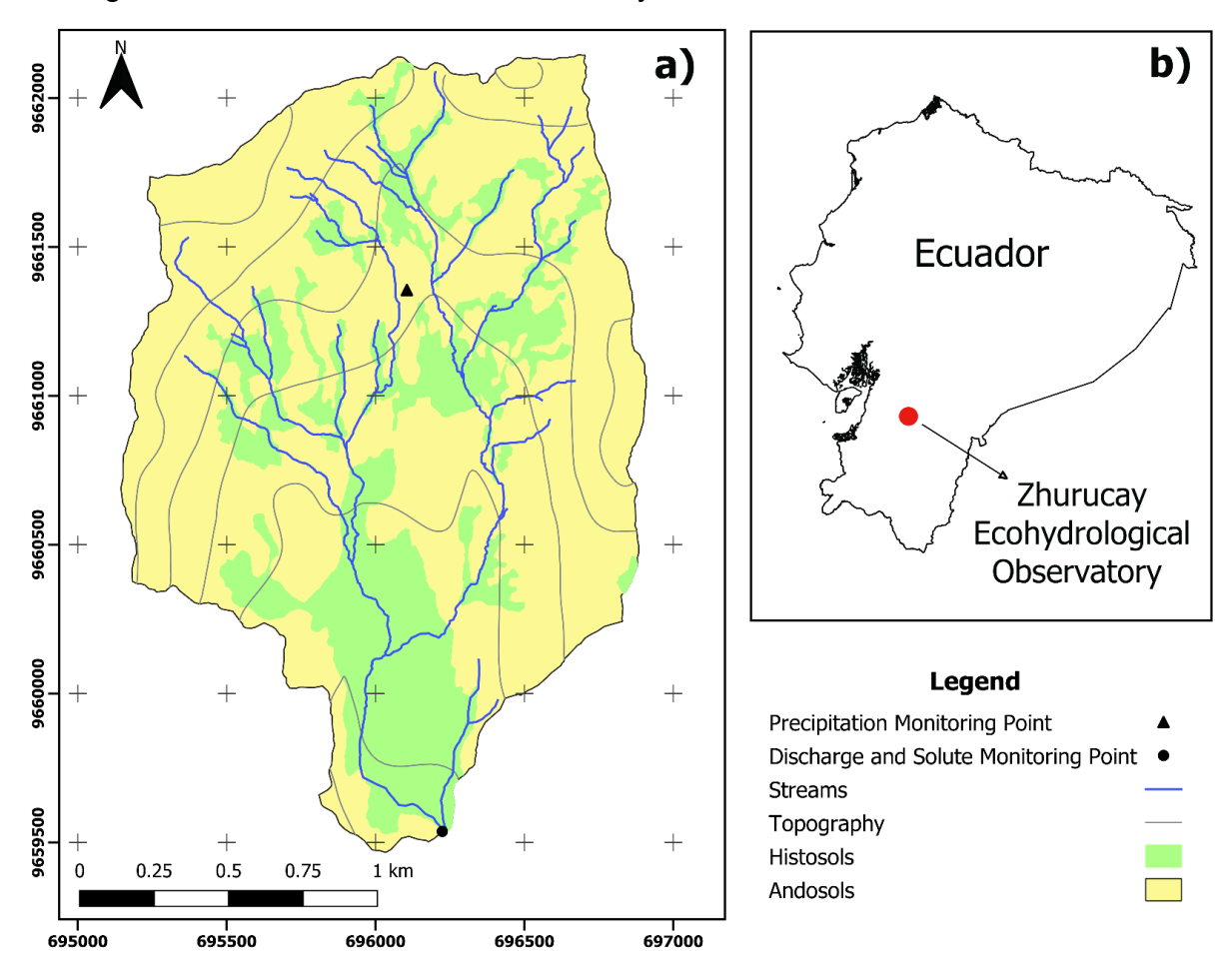


**Figure 1.** Zhurucay experimental catchment, highlighting a) the distribution of the streams, the two main types of soil (Histosols, Andosols), besides the position of the monitoring points of precipitation and discharge/solute chemistry at the microcatchment outlet, and b) its location on the Ecuadorian geography.

The primary geological components of the catchment are the late Miocene formations of Quimsacocha (basaltic flows with plagioclases, feldspars, and andesitic pyroclastics) and Turi (tuffaceous andesitic breccias, conglomerates, and horizontal stratified sands) (Pratt et al., 1997). These quaternary formations were deposited as a result of the volcanic and glacial activity that occurred during the last Ice Age (Coltorti & Ollier, 2000; Hungerbühler et al., 2002).

According to the FAO soil classification system, ZEO is composed by two main soil types (Histosols and Andosols) which cover respectively 22% and 78%, of the total catchment area (Crespo et al., 2011; Mosquera et al., 2015). These types of soils are strongly acid (pH ≈ 4.8), rich in organic matter content, and highly porous-attributes that give them a great water-retention capacity. Histosols are located mostly at valley bottoms reaching depths of 24 to 70 cm (Buytaert & Beven, 2011) and their usual vegetation cover is composed of Cushion plants (*Plantago rigida, Xenophyllum humile, Azorella* spp.), mosses, and lichens (Ramsay & Oxley, 1997; Sklenar & Jorgensen, 1999). On the other hand, Andosols are located mostly on valley slopes, show relatively little horizon development, ranging from 24 to 44 cm (Buytaert et al., 2006). Andosols vegetation consists regularly of herbaceous plants, such as tussock grass (*Calamagrostis sp.*) (Ramsay & Oxley, 1997; Sklenar & Jorgensen, 1999).

#### 2.2 Data Collection

During the intensive monitoring campaign carried out in the study area from March 2018 to March 2019, discharge data was collected at the catchment outlet. A V-notch weir was used to record water level measurements at a five minutes frequency, by means of a submerged AquiStar CT2X smart sensor with pressure option (Accuracy = ±0.06%) (Instrumentation Northwest, Inc., Denver, Colorado, USA). These readings were then transformed into flow rates via a calibrated discharge curve based on the Kindsvater-Shen relationship (U.S. Bureau of Reclamation, 2001). The curve was calibrated by means of salt dilution techniques (Moore, 2004).

Precipitation information used in this study was taken from a continuous monitored system settled in the climatic main station, located at the upper part of the ZEO. The equipment in charge of these measurements is a Texas Electronics tipping-bucket rain gauge (TR-525M, Dallas, TX, USA), with a resolution of 0.1 mm and a 5-minute frequency.

Solute chemical data was also monitored for an entire year (March 2018-March 2019), in order to capture the seasonal variability of its behavior, which is a key factor for the hysteresis analysis that would be performed. To assess water quality, we installed a UV-Visible Spectrometer Probe V2 (Spectrolyser, s::can Messtechnik GmbH, Vienna, Austria) at the catchment outlet to infer concentrations of the following constituents: aluminum (AI), copper (Cu), dissolved organic carbon (DOC), total bound nitrogen (TNb), barium (Ba), calcium (Ca), magnesium (Mg), sodium (Na), strontium (Sr), potassium (K), silicon (Si), and rubidium (Rb) at a high (5-minute) time resolution. These concentrations were validated using calibration functions based on principal components regressions, comparing indirect and direct measurements (Pesántez et al., 2021).

#### 2.3 Storm Analysis

We initially employed the discharge time-series graph to identify individual hydrological events. We used the Peak-Over-Threshold (POT) principle, which consists in retaining all peak discharge values that exceed a selected threshold, defining single hydrological events (Lang et al., 1999). To set the POT threshold, we used the 30<sup>th</sup> percentile of the discharge range (considered as the baseflow rate). This procedure was carried out thanks to the R package POT (Ribatet & Dutang, 2018). During the wet season, the presence of extreme flow rates caused hydrological events with multiple peaks. In these cases, we considered each peak flow as a separated event in order to quantify the solute response to each separated event, following the methodology presented by Lloyd et al. (2016a).

To gain insights into hydrologic seasonal behavior of the catchment, event flow rates were grouped into three classes: high-flow, mid-flow, and low-flow. Using the flow duration

curve (FDC) and following the criteria proposed by Mosquera et al. (2015), we defined high-flow category with discharge values that exceed the 90 percent frequency of non-exceedance ( $>Q_{90}$ ), mid-flow with values between the 30 percent and 90 percent ( $Q_{30}$  -  $Q_{90}$ ) and low-flow category was set with values below the 30 percent frequency of non-exceedance ( $<Q_{30}$ ).

Besides the flow categorization, we classified each storm event according to its chemical status: dilution, chemostasis, or mobilization (Basu et al., 2010; Clow & Mast, 2010; Godsey et al., 2009). A chemostasis stage implies that the regression line to the log-solute concentration (log-C) vs. log-discharge (log-Q) fit has a zero slope. A positive slope of the regression line points mobilization behaviors (enrichment), on the other hand, a negative slope indicates dilution characteristics. This classification will let us characterize hydrological and biogeochemical behaviors at event scale of a varied range of solutes considered in this work.

In addition to the previous categorizations, each event was quantitative described through the calculation of the following precipitation, concentration and discharge variables *(Table 1)*.

**Table 1** Computed storm variables describing hydrological behavior at an event scale. They are hypothesized to be potential controlling factors of water quality. Mean, max and min stands for the variable average, maximum and minimum magnitude, respectively. Mean 24, 48, 72, 96 and 120 represents the average magnitude of the variable 24, 48, 72, 96 and 120 hours before the event, respectively. Range denotes the difference between max and min.

#### STORM VARIABLES

Precipitation	Concentration	Discharge
Mean	Max	Duration
Mean 24	Min	Max
Mean 48	Range	Min
Mean 72	Mean	Range
Mean 96		Mean
Mean 120		Mean 24
Cumulated		



#### 2.4 Hysteresis Loop Characterization

Concentration-discharge loops were constructed for each hydrological event. These were classified in a quantitative way (by shape), following a C-Q criteria in classes I, II, III, IV and V (Williams, 1989). Class I (direct) is characterized by a direct response whereby solute concentrations increase or decrease proportional to flow rates, indicating an uninterrupted supply of particles during the hydrological event (Walling & E., 1974; Williams, 1989). Class II (clockwise) hysteresis is characterized by a faster increase in concentration rates than in discharge ones, suggesting that the sources of runoff are located close to the monitoring point (Walling & E., 1974; Williams, 1989; Wood, 1977). Class III (anti-clockwise) hysteresis may exist as a result of an extended lag between the concentration and discharge peaks, it signifies that the sources of runoff are located far from the monitoring point (C. Evans & Davies, 1998; Heidel, 1956; Williams, 1989). Class IV hysteresis is a combination of class I and class II or III, whereby the solute concentrations vary similarly to the water discharge rates at the beginning and end of the hydrograph, but flow peaks may produce a lag between C-Q responses, causing typical clockwise or anticlockwise shaped loops. There is no clear idea about the circumstances that may trigger class IV hysteresis response, given that a very little literature was found about this topic (Williams, 1989). Finally, class V (figure-eight) hysteresis combines classes II and III, whereby the C-Q patterns are represented by a clockwise loop for high flows and a counterclockwise loop for low flows pointing to a possible heterogeneous evolution in the export of solute concentrations (Arnborg et al., 1967; Seeger et al., 2004; Williams, 1989).

The above explained hysteresis classification is prone to subjective interpretations, especially for complex hysteresis loops such as classes II, III, and V which is why a quantitative classification is required (Bowes et al., 2015; Butturini et al., 2008; C. Evans & Davies, 1998). The hysteresis index (HI), proposed by Lloyd et al. (2016b), helped us to carry out this quantitative classification. They present a robust method for obtaining HI, using the range of solute concentration values between the rising and falling limbs at

multiple percentiles of discharge. In addition, to have a complete characterization of the whole loop shape, we took multiple HI measurements during the same storm (one HI for each 5th percentile range of discharge).

In the HI calculation process, the first step is to normalize the discharge and solute concentration information:

$$Norm. Q_i = \frac{Q_i - Q_{min}}{Q_{max} - Q_{min}}, \tag{1}$$

$$Norm. C_i = \frac{C_i - C_{min}}{C_{max} - C_{min}}, \tag{2}$$

where  $Q_i/C_i$  is the discharge/solute concentration at timestep i,  $Q_{min}/C_{min}$  is the minimum discharge/solute concentration value, and  $Q_{max}/C_{max}$  is the maximum discharge/solute concentration value. HI is then calculated as follows:

$$HI_{Q_i} = C_{RL_Q_i} - C_{FL_Q_i}, \tag{3}$$

where  $HI_{Q_i}$  is the hysteresis index at percentile i of discharge,  $C_{RL\_Q_i}$  is the solute concentration on the rising limb at percentile i of discharge, and  $C_{FL\_Q_i}$  is the solute concentration at the equivalent point in discharge on the falling limb.

With regard to the percentiles of discharge  $(Q_i)$  calculation:

$$Q_i = k(Q_{max} - Q_{min}) + Q_{max}, (4)$$

where  $Q_{max}$  is the peak discharge,  $Q_{min}$  is the discharge at the start of the event, and k is the point along the loop at which the HI is calculated.

In our specific case, HI was calculated at every 5th percentile of discharge, that is: k = 0.05, 0.1, 0.15, ..., 0.95. One of the most important benefits of calculating HI is that the results, which vary between -1 and 1, are easy to interpret. The larger the HI value, the

"fatter" the loop—so that when the HI value is close to 0, the shape of the loop resembles a figure eight. The HI indicates the direction of the loop: positive (+) signifies a clockwise loop, and negative (-) an anti-clockwise loop.

To ensure an effective hysteresis characterization, an additional descriptor was computed for each hysteresis loop, the loop area, which varies between 0 and 1 thanks to the normalized data. In conjunction with HI, loop area helps clarify the amplitude and strength of the hysteresis loop.

#### 2.5 Analysis of the Hysteresis Indicators Variability Controls

To analyze how and which storm variables affect the solute concentration dynamics, we carried out a correlation analysis of the relationship between the storm variables (precipitation, concentration and discharge), and the hysteresis descriptors (HI, loop and area). The results will be reported as Spearman correlation values (r), which vary between —1 and 1, indicating negative or positive associations, respectively.

Because of the clear necessity of identifying complex relationships, connections, patterns and controllers of HI variability, in addition to the non-normal distribution (p < 0.05) of precipitation, concentration, and discharge variables, we decided to use the Classification and Regression Trees (CART) method (Breiman et al., 1984) implemented in the R package rpart (Therneau & Atkinson, 2019), together with the Spearman correlation analysis. CART technique provides a description of HI variability through an iterative division process, storm variables (precipitation, concentration and discharge) are split into two subgroups each time until the two most homogenous satisfy a predefined binary condition.

With the objective of ranking storm variables according to their impact on HI variability, we employed a random forest (RF) analysis based on the CART method and implemented in the R package randomForest (Liaw & Wiener, 2002). Increased mean square error (IncMSE) and increased impurity index (IncNodePurity) were applied as a quantitative way to point the hierarchical storm variables importance. The first one deals with the



effects on the storm variable-HI interaction when storm variables are randomly permuted, the second one shows the homogeneity growth carried every time a partitioning is done. Consequently, as IncMSE and IncNodePurity increase, the storm variable importance/impact on HI variability increases too.

#### 3. Results

#### 3.1 Storm Analysis

Throughout the study period, 85 individual hydrological events were identified and characterized according to the descripting variables of precipitation, concentration and discharge (*Table 1*, *Table 2*). 29 events (34.12 %) presented high flow rates, 36 (42.35 %) mid flow rates and 20 (23.53 %) low flow rates. Considering event chemical status, we found that some solutes, such as Ba, Cu, Ca, Mg, Al, DOC, and TNb show a strong predominance of mobilization events (83.53 % - 95.29 %). On the other hand, solutes like Na, Sr, K, Si, and Rb mostly presented dilution events (60 % - 83.53 %). Chemostatic events were rarely found, appeared in the following solutes: Sr (3.53 %), Na (7.06 %), Ca (3.53 %), and Mg (4.71 %).

**Table 2** Summary statistics of the 85 events identified, in each event variables of precipitation, concentration and discharge were calculated. Mean, Max and Min stands for the variable average, maximum and minimum magnitude, respectively. Mean 24, 48, 72, 96 and 120 represents the average magnitude of the variable 24, 48, 72, 96 and 120 hours before the event, respectively. Range denotes the difference between Max and Min.

		Min	Max	Mean	Median	Stand. Dev.
	Mean (mm/h)	0.001	0.158	0.023	0.016	0.022
	Mean 24 (mm/h)	0.000	0.078	0.022	0.018	0.019
	Mean 48 (mm/h)	0.000	0.063	0.019	0.015	0.015
<b>Precipitation</b>	Mean 72 (mm/h)	0.000	0.067	0.018	0.015	0.014
	Mean 96 (mm/h)	0.000	0.058	0.017	0.015	0.012
	Mean 120 (mm/h)	0.001	0.047	0.016	0.015	0.011
	Cumulated (mm)	2.663	68.166	26.500	23.688	15.128

	Max (ppm)	0.162	0.740	0.398	0.392	0.147
_	Min (ppm)	0.000	0.455	0.195	0.183	0.095
Al –	Range (ppm)	0.037	0.555	0.203	0.168	0.131
_	Mean (ppm)	0.106	0.600	0.295	0.277	0.110
	Max (ppm)	0.007	0.023	0.013	0.012	0.004
_	Min (ppm)	0.004	0.015	0.009	0.009	0.002
Cu -	Range (ppm)	0.001	0.012	0.004	0.003	0.003
_	Mean (ppm)	0.006	0.019	0.011	0.010	0.003
	Max (ppm)	0.042	3.214	1.353	1.302	0.799
	Min (ppm)	0.000	1.864	0.486	0.343	0.506
DOC -	Range (ppm)	0.042	2.488	0.867	0.790	0.659
_	Mean (ppm)	0.009	2.539	0.906	0.791	0.606
	Max (ppm)	0.038	3.253	1.352	1.295	0.806
_	Min (ppm)	0.000	1.865	0.483	0.340	0.505
TNb -	Range (ppm)	0.038	2.502	0.869	0.788	0.665
_	Mean (ppm)	0.007	2.556	0.902	0.786	0.608
	Max (ppm)	0.007	0.063	0.042	0.040	0.007
-	Min (ppm)	0.032	0.046	0.042	0.040	0.007
Ba -	Range (ppm)	0.027	0.040	0.008	0.007	0.004
_		0.002	0.022	0.003	0.007	0.005
	Mean (ppm) Max (ppm)	1.863	3.481	2.384	2.313	0.005
_		1.585	2.364	1.972	1.920	0.330
Ca -	Min (ppm)	0.092	1.146	0.412	0.317	0.180
_	Range (ppm)	1.719		2.138	2.072	0.234
	Mean (ppm)		2.805			
_	Max (ppm)	0.506	0.892	0.638	0.619	0.083
Mg -	Min (ppm)	0.414	0.629	0.521	0.514	0.049
_	Range (ppm)	0.034	0.284	0.116	0.096	0.072
	Mean (ppm)	0.458	0.709	0.570	0.554	0.054
_	Max (ppm)	1.997	4.546	3.175	3.138	0.477
Na -	Min (ppm)	1.432	3.479	2.385	2.372	0.451
_	Range (ppm)	0.222	2.415	0.789	0.664	0.508
	Mean (ppm)	1.743	3.773	2.736	2.720	0.380
_	Max (ppm)	0.040	0.100	0.061	0.059	0.011
Sr -	Min (ppm)	0.029	0.068	0.045	0.045	0.009
_	Range (ppm)	0.004	0.061	0.016	0.012	0.012
	Mean (ppm)	0.034	0.075	0.051	0.050	0.008
_	Max (ppm)	0.552	1.386	0.925	0.912	0.160
<b>K</b> -	Min (ppm)	0.285	1.039	0.613	0.597	0.173
	Range (ppm)	0.101	0.872	0.312	0.275	0.187
	Mean (ppm)	0.454	1.108	0.763	0.766	0.134
Si -	Max (ppm)	6.176	15.476	11.073	11.112	1.975
O1	Min (ppm)	2.358	12.324	7.615	7.577	2.314

Concentration



		Range (ppm)	0.828	10.366	3.458	2.929	2.372
	-	Mean (ppm)	5.408	13.018	9.150	9.402	1.896
		Max (ppm)	0.000	0.003	0.002	0.002	0.001
	Rb ·	Min (ppm)	0.000	0.002	0.001	0.001	0.001
	KD	Range (ppm)	0.000	0.002	0.001	0.001	0.001
		Mean (ppm)	0.000	0.002	0.001	0.001	0.000
		Duration (h)	3.167	222.833	25.681	19.500	28.795
		Max (L/s)	23.110	1952.180	316.090	183.340	386.647
Diocharga		Min (L/s)	19.980	556.950	103.605	84.060	102.454
Discharge		Range (L/s)	1.560	1701.230	212.485	74.115	341.703
		Mean (L/s)	21.624	760.935	161.884	106.622	162.365
		Mean 24 (L/s)	9.245	452.842	104.393	79.127	93.629

#### 3.2 Hysteresis Loop Characterization

Using the quantitative approach (HI), we classified each hydrological event into four main hysteresis categories: clockwise, anti-clockwise, direct, and figure 8. In order to validate this quantitative hysteresis classification, every single hydrological event was visually inspected (qualitative approach). As we see in *Figure 2*, solutes can be grouped into three classes: anti-clockwise dominance (ACD: AI, Cu, DOC and TNb), clockwise dominance (CD: Na, Sr, K, Si and Rb) and the last one has mixed presences of the four hysteresis types (M: Ba, Ca and Mg). What is interesting here is the presence of a few clockwise events in the anti-clockwise domain group (Cu, DOC and TNb), situation not reciprocal in clockwise domain group.

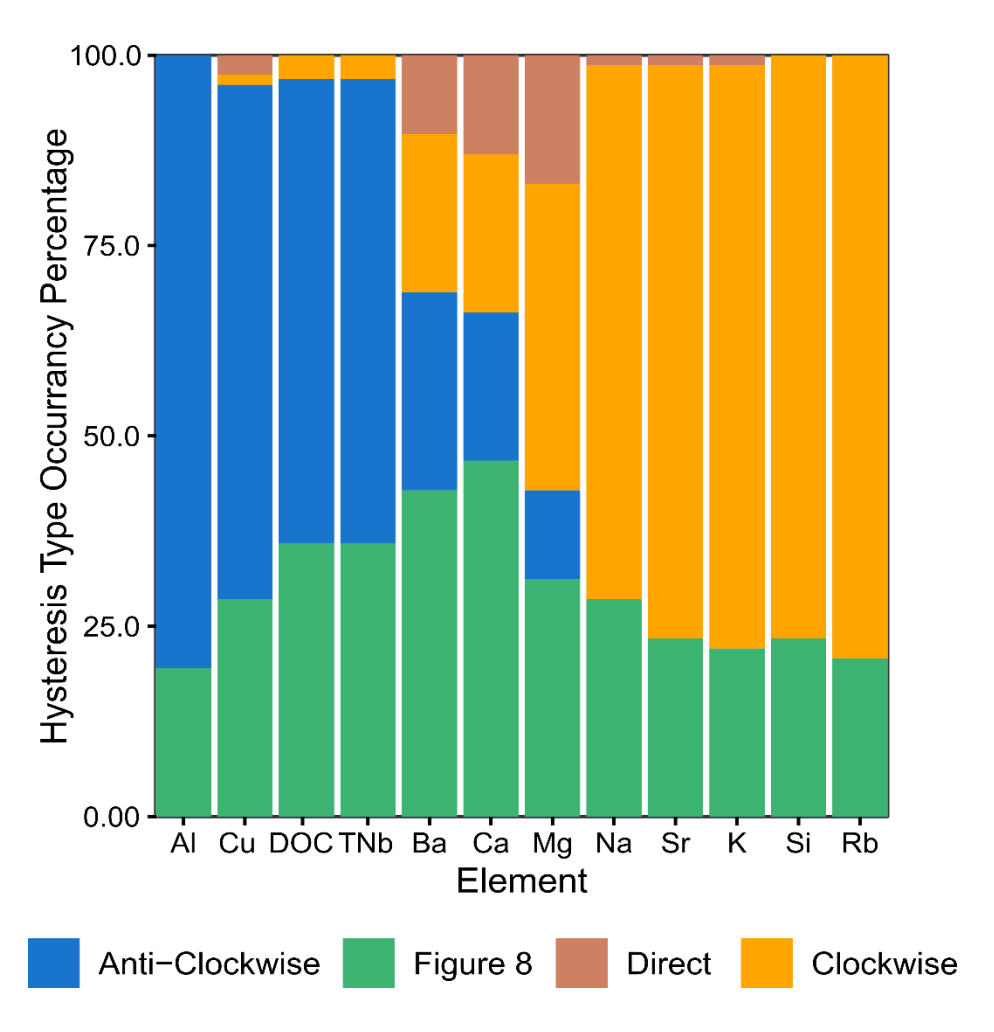


**Figure 2** Hysteresis loop types occurrancy percentage in each element, for the 85 individual hydrological events identified.

There is a constantly presence of figure 8 hysteresis type. At least, 20% of the events, present this shape for all the solutes. Direct responses represent a minimal portion of the hysteresis types distribution, especially in clockwise dominance group, and its major occurrence appears in Mg (≈20 %). In order to exemplify the type of hysteresis found, we selected one representative solute for each dominance group, that is DOC for anticlockwise dominance, Na for clockwise dominance and Ca for the mixed group. *Figure 3* shows us the hysteresis response of the mentioned solutes to two different hydrological events, for the first hydrological event, the three solutes show a figure 8 hysteresis response. DOC and Na hysteresis loops have similar shapes and areas but opposite directions. If we compare Na and Ca hysteresis loops, we can appreciate similar

directions, however, Ca loop has a better-defined shape. The second hydrological event displays us the typical response for each dominant group: DOC – anti-clockwise, Na – clockwise, and Ca – direct.

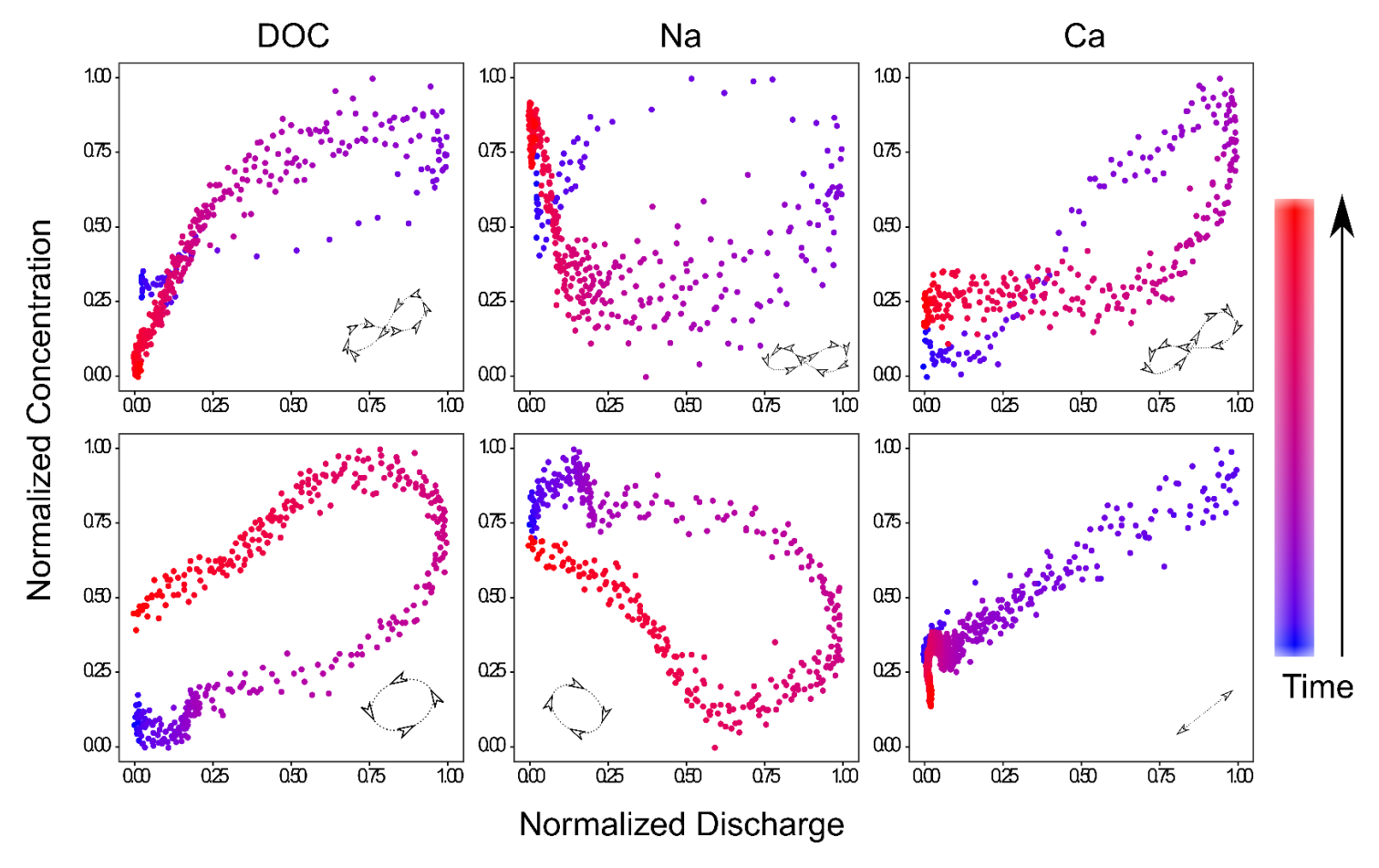


**Figure 3** Two hydrological events with different hysteresis responses according to each element. In this case, we used DOC, Na and Ca as an exemplification of the three groups: anti-clockwise domain, clockwise domain and mixed, respectively. Both discharge and concentration were normalized using the methodology proposed by Lloyd et al. (2016b). A graphic scheme of the loop direction was added in each loop in order to improve its assimilation.

#### 3.3 Analysis of the Hysteresis Indicators Variability Controls

Out of the total of 85 events analyzed, we identified which of them corresponded to mobilization, which to dilution and which to chemostatic chemical status. Results were



graphed along the hydrograph of the studied period (*Figure 4*), solutes from the anticlockwise (DOC), clockwise (Na), and mixed dominance group (Ca) were selected in order to point out the evolution of the event chemical status through time. The majority of DOC and Ca events exhibits a mobilization chemical status. On the other hand, most of Na events show dilution tendencies with the presence of a few chemostasis and mobilization events.

Both Spearman correlation and random forest analysis (Table 3 and Table 4) were developed to find the hydrometeorological controllers (precipitation, concentration and discharge) of the hysteresis indicators (HI and loop area) variability. Regarding HI, as can be seen from Table 3, precipitation variables do not exhibit close relationships with HI variability, excluding punctual cases such as mean precipitation and mean 120 that point some influence on Na, Sr, Cu, and Ba according to the Spearman correlation values (r) and top-ranking values of random forest (RFI). Checking out r values at concentration variables, we can find considerably relationships with HI variability from range of concentration and max concentration, principally with certain solutes of the clockwise domain group (Na, Sr, K). Typically, anti-clockwise solutes (DOC, TNb) indicate high relative r values with max concentration and Ca, Mg (mixed group) with range of concentration. However, RFI ranking shows that just a few solutes find concentration variables as the most important ones to HI variability, those solutes are DOC, TNb, and Na (max, range and mean). A closer inspection to the table reveals that range of discharge, max discharge, and mean discharge represent the most important variables to the HI variability, according to RFI. Also, the highest r values match with the top-ranking RFI values, mostly. It is important to mention two interesting facts here, the first one is that event duration has a moderate impact on Si and Rb, given that their r values are relatively high (-0.246 and -0.247) compared to other solutes r values. The second one is that the clockwise domain group is negative correlated with discharge variables. Besides the highranking RFI values that Na, Sr, and K (clockwise group) show at discharge variables, r correlation values suggest a greater influence of concentration variables.

Respecting loop area (*Table 4*), we realize that precipitation variables gained more importance, particularly in antecedent precipitation (mean 72, 96, 120) to solutes like Ba and Ca that belong to the mixed dominance group. Correlation values of concentration variables remain similarly to r values featured in *Table 3*, with the biggest impact performed by max concentration. Discharge variables remain more significant than concentration and precipitation variables to the loop area variability, according to both random forest and correlation processes.

Considering the previous statements about the relationships between event variables and hysteresis indicators variation, we set discharge variables as the most influencing ones to HI variation followed by concentration variables and finally precipitation variables that surprisingly not exert greater influence.

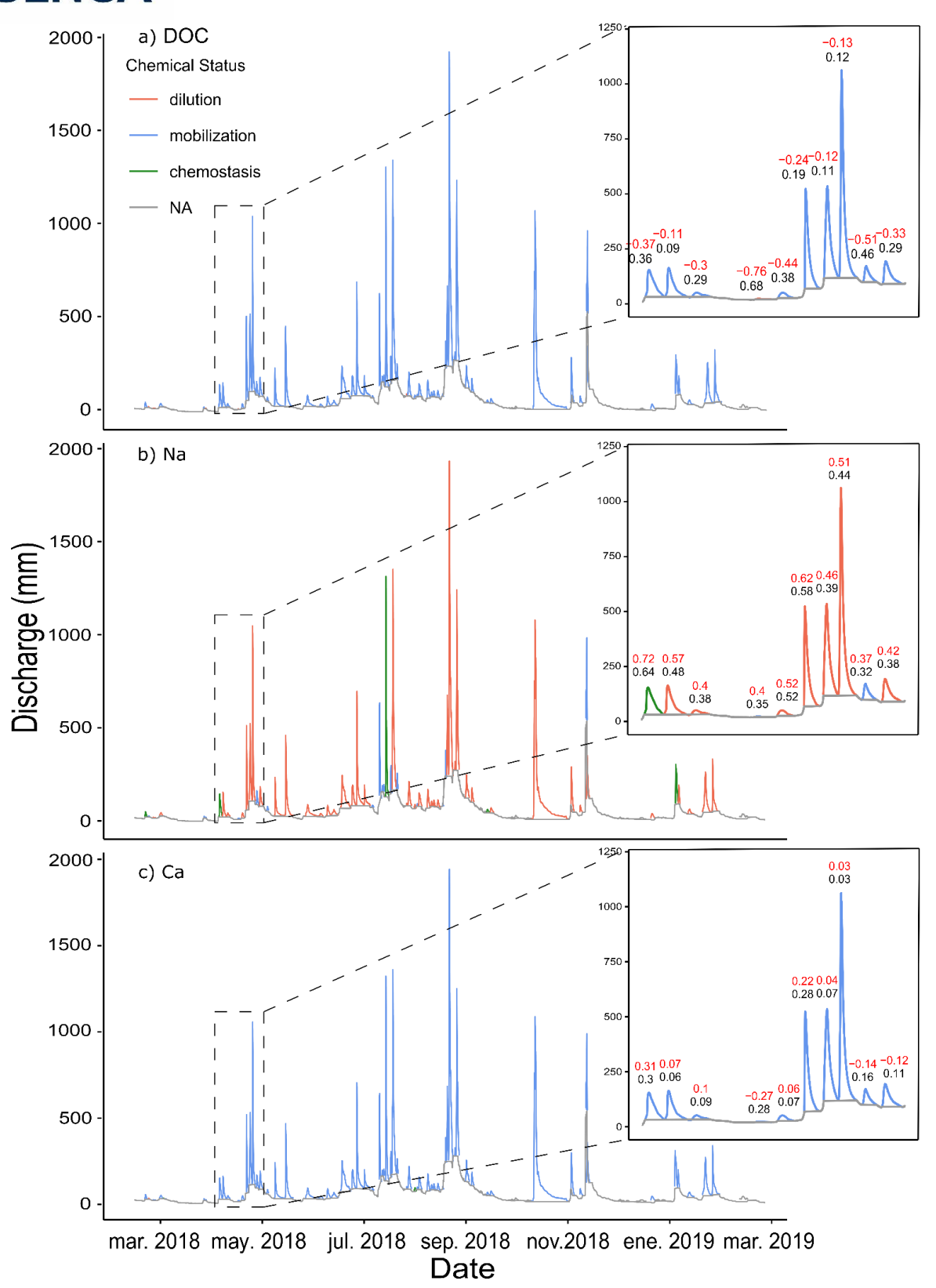


**Figure 4** Chemical status categorization of the study period hygrogram for a) DOC, b) Na and c) Ca. Zoom boxes indicate specific events where HI (red) and loop area (black) values were placed for each one.

**Table 3** Summary of the random forest and correlation analysis between the event variables (precipitation, concentration, discharge) and the calculated hysteresis index (HI). Random forest results are shown as an importance ranking of the event variables (RFI) and the correlation results are shown as values of the Spearman correlation coefficient (r). Max and Min stand for the variable average, maximum and minimum magnitude, respectively. Mean 24, 48, 72, 96 and 120 represents the average magnitude of the variable 24, 48, 72, 96 and 120 hours before the event, respectively. Range denotes the difference between Max and Min.

		Precipitation								Conce	ntration		Discharge					
		Mean	Mean 24	Mean 48	Mean 72	Mean 96	Mean 120	Accumulated	Max	Min	Range	Mean	Duration	Max	Min	Range	Mean	Mean 24
Al	RFI	17	13	15	16	14	11	9	5	6	8	7	12	2	10	1	4	3
AI	r	0.078	0.120	0.102	0.115	0.087	0.109	0.143	0.278	0.330	0.072	0.223	0.197	0.455	0.285	0.429	0.402	0.245
Cu	RFI	17	14	15	9	11	3	16	4	8	7	10	13	2	12	1	6	5
Cu	r	-0.018	0.171	0.119	0.120	0.092	0.135	0.067	0.314	0.216	0.232	0.204	0.235	0.463	0.158	0.477	0.341	0.185
DOC	RFI	7	17	16	14	15	13	6	1	11	4	3	12	5	10	2	8	9
ВОС	r	0.031	0.208	0.139	0.112	0.047	0.096	-0.003	0.483	0.275	0.374	0.341	0.272	0.478	0.141	0.498	0.340	0.071
TNb	RFI	10	17	12	15	14	13	5	2	8	3	4	16	6	11	1	7	9
IND	r	0.029	0.204	0.137	0.110	0.045	0.094	-0.005	0.477	0.273	0.372	0.336	0.273	0.478	0.142	0.498	0.341	0.070
	RFI	16	12	15	5	4	2	10	9	14	7	11	17	3	8	1	6	13
Ва	r	0.388	0.172	0.097	0.098	0.054	0.064	0.115	0.312	0.061	0.350	0.130	0.192	0.526	0.383	0.481	0.507	0.074
0-	RFI	13	15	16	10	4	5	11	8	12	7	14	17	1	6	3	2	9
Ca	r	0.257	0.130	-0.047	-0.044	-0.055	-0.041	0.091	0.191	-0.230	0.377	-0.056	0.215	0.395	0.256	0.370	0.359	-0.045
Ma	RFI	16	9	15	11	8	4	13	12	14	5	10	17	2	6	3	1	7
Mg	r	0.246	0.190	0.064	0.047	0.007	0.005	0.078	0.190	-0.300	0.422	-0.085	0.200	0.378	0.180	0.374	0.310	-0.009
N-	RFI	12	16	14	11	17	15	8	10	6	2	13	9	3	5	1	4	7
Na	r	0.103	0.003	0.005	-0.055	-0.082	-0.103	0.053	0.171	-0.101	0.250	-0.062	-0.099	-0.032	-0.016	-0.031	-0.003	-0.048
0	RFI	11	14	17	13	16	9	8	15	6	4	12	10	2	5	1	3	7
Sr	r	0.137	0.066	0.053	-0.016	-0.040	-0.057	0.061	0.187	-0.138	0.281	-0.065	-0.057	0.054	-0.009	0.063	0.042	-0.054
	RFI	13	16	15	14	17	12	10	5	7	8	9	11	2	6	1	3	4
K	r	0.022	-0.043	-0.082	-0.124	-0.126	-0.149	-0.071	0.360	0.120	0.198	0.173	-0.100	-0.197	-0.173	-0.172	-0.191	-0.188
0:	RFI	12	17	15	14	13	16	7	11	10	6	5	4	2	9	1	3	8
Si	r	0.082	-0.098	0.000	-0.035	-0.031	-0.059	0.070	0.110	0.025	0.067	-0.033	-0.246	-0.210	-0.007	-0.235	-0.099	-0.046
	RFI	15	17	16	13	12	11	9	8	10	14	7	4	2	5	1	3	6
Rb	r	0.073	-0.112	-0.051	-0.077	-0.057	-0.091	0.041	0.189	0.119	0.061	0.041	-0.247	-0.238	-0.077	-0.246	-0.158	-0.085

\*RFI = Random Forest Importance \*r = Spearman correlation value \* Colors blue, coral and purple were assigned to the first, second and third highest r relative values, respectively. Same color scheme was used to the top three RFI values (1, 2, 3)

**Table 4** Summary of the random forest and correlation analysis between the event variables (precipitation, concentration, discharge) and the calculated loop area. Random forest results are shown as an importance ranking of the event variables (RFI) and the correlation results are shown as values of the Spearman correlation coefficient (r). Max and Min stand for the variable average, maximum and minimum magnitude, respectively. Mean 24, 48, 72, 96 and 120 represent the average magnitude of the variable 24, 48, 72, 96 and 120 hours before the event, respectively. Range denotes the difference between Max and Min.

		Precipitation								Concentration				Discharge					
		Mean	Mean 24	Mean 48	Mean 72	Mean 96	Mean 120	Accumulated	Max.	Min.	Range	Mean	Duration	Max.	Min.	Range	Mean	Mean 24	
Al	RFI	17	11	14	16	13	9	15	6	3	8	7	12	5	10	2	4	1	
	r	-0.073	-0.116	-0.148	-0.142	-0.121	-0.139	-0.197	-0.358	-0.373	-0.131	-0.280	-0.247	-0.496	-0.316	-0.466	-0.444	-0.309	
Cu	RFI	17	14	13	8	9	3	15	4	10	6	12	11	2	16	1	7	5	
	r	0.037	-0.138	-0.167	-0.151	-0.134	-0.170	-0.092	-0.393	-0.210	-0.331	-0.236	-0.335	-0.466	-0.188	-0.471	-0.349	-0.197	
DOC	RFI	16	15	12	14	17	13	7	1	9	3	2	6	5	10	4	8	11	
	r	-0.080	-0.184	-0.203	-0.147	-0.093	-0.135	-0.082	-0.635	-0.311	-0.531	-0.447	-0.350	-0.553	-0.221	-0.559	-0.422	-0.138	
TNb	RFI	11	16	13	12	15	17	6	1	9	2	4	7	5	14	3	8	10	
	r	-0.077	-0.181	-0.202	-0.146	-0.093	-0.134	-0.080	-0.629	-0.310	-0.528	-0.444	-0.347	-0.550	-0.221	-0.556	-0.421	-0.135	
Ва	RFI	15	14	12	3	2	1	6	8	13	16	9	17	5	11	7	4	10	
	r	0.224	-0.236	-0.340	-0.402	-0.446	-0.493	0.020	0.035	0.002	0.042	0.072	0.014	0.209	0.236	0.165	0.270	-0.036	
Ca	RFI	15	14	13	9	10	5	6	16	8	11	17	12	3	7	1	2	4	
Ca	r	0.211	-0.061	-0.202	-0.236	-0.284	-0.310	0.087	0.071	0.030	0.069	0.066	0.015	0.178	0.201	0.142	0.219	-0.058	
Mg	RFI	16	15	13	11	2	1	8	5	3	9	7	17	10	14	6	12	4	
wig	r	0.276	0.015	-0.139	-0.145	-0.204	-0.256	-0.040	0.176	-0.153	0.305	0.013	0.159	0.305	0.139	0.304	0.250	-0.151	
Na	RFI	12	16	15	14	17	13	9	6	8	1	11	10	2	5	3	4	7	
INA	r	0.093	0.033	-0.017	-0.049	-0.072	-0.093	0.007	0.258	-0.079	0.312	0.002	-0.050	-0.036	-0.056	-0.024	-0.041	-0.115	
Sr	RFI	15	11	17	14	16	13	10	8	7	3	9	12	1	5	4	2	6	
31	r	0.158	0.090	0.025	-0.007	-0.026	-0.041	0.012	0.269	-0.114	0.342	-0.006	-0.018	0.051	-0.049	0.073	0.006	-0.123	
K	RFI	12	16	17	15	14	13	11	3	8	6	9	10	1	7	2	5	4	
N.	r	0.015	-0.026	-0.109	-0.123	-0.125	-0.151	-0.112	0.444	0.149	0.242	0.231	-0.057	-0.194	-0.207	-0.158	-0.221	-0.243	
Si	RFI	15	17	16	14	12	13	9	10	11	6	8	4	1	7	2	3	5	
SI	r	0.063	-0.053	-0.004	-0.013	-0.013	-0.039	0.013	0.208	0.092	0.084	0.050	-0.249	-0.258	-0.067	-0.272	-0.170	-0.130	
Dh	RFI	15	16	17	14	9	12	10	4	13	11	7	2	3	8	1	5	6	
Rb	r	0.077	-0.077	-0.064	-0.063	-0.050	-0.082	-0.020	0.277	0.185	0.080	0.110	-0.256	-0.275	-0.129	-0.273	-0.219	-0.171	

\*RFI = Random Forest Importance \*r = Spearman correlation value \* Colors blue, coral and purple were assigned to the first, second and third highest r relative values, respectively. Same color scheme was used to the top three RFI values (1, 2, 3)

In order to examine in a better way, the relationships between storm events behavior and hysteresis response variability, scatter plots were built. X-axis of these graphs are taken by storm variable values (discharge mainly) and Y-axis denotes the hysteresis indicators. Because of their relative high r and RFI values, range of discharge (*Figure 5*), was selected in this plot.

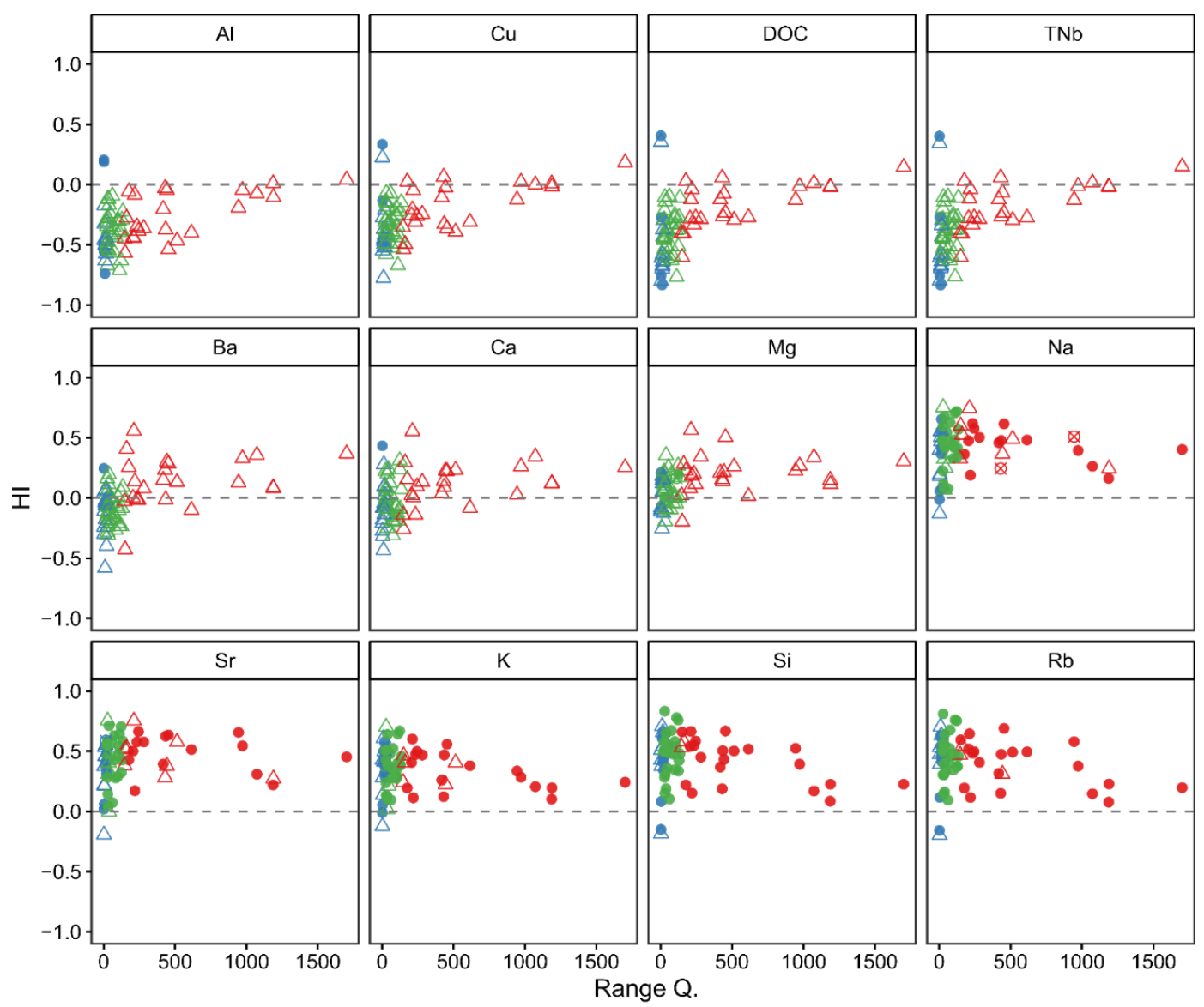


**Figure 5** Visual relationships between range of discharge (Range Q.) and the calculated hysteresis index (HI) for each element. A dot represents a single hydrological event and it is categorized according to its chemical state (shape: chemostasis, dilution, mobilization) and its flow rate (color: high, mid, low). The solutes are ordered according to anti-clockwise domain, mixed and clockwise domain classification, respectively.

**Figure 5** provides an overview of the range of discharge (Range Q) and the Hysteresis Index (HI) for each solute considered in this study. What stands out in the figure is when the range of discharge magnitude increases (high-flow rates), HI tends to 0, meaning that the loop shape tends to a low-area figure 8 or a direct response. To low-flow and midflow rates, there is no clear relationship between range of discharge and HI. HI is highly variable at those conditions.

It seems that the anti-clockwise domain (AI, Cu, DOC and TNb) and mixed group (Ba, Ca and Mg) show dilution chemical states at low-flow discharge rates (however, there are a few events that display a mobilization behavior), mid-flow and high-flow discharge rates correspond to mobilization chemical states (*Figure 5*). On the other hand, clockwise domain solutes (Na, Sr, K, Si and Rb) seem to have an opposite behavior: mobilization at low-flow rates and dilution at mid-flow and high-flow (*Figure 5*). Nevertheless, we can find a few events that exhibit mobilization chemical states at mid-flow and high-flow discharge rates, or dilution at low-flow rates. It is hard to visualize chemostasis behaviors, except for Na at high-flow discharge rates (*Figure 5*). Indeed, just a few events have chemostasis status and we suspect that it is more likely to be found at low-flow rates for Na, Ca, and Mg.

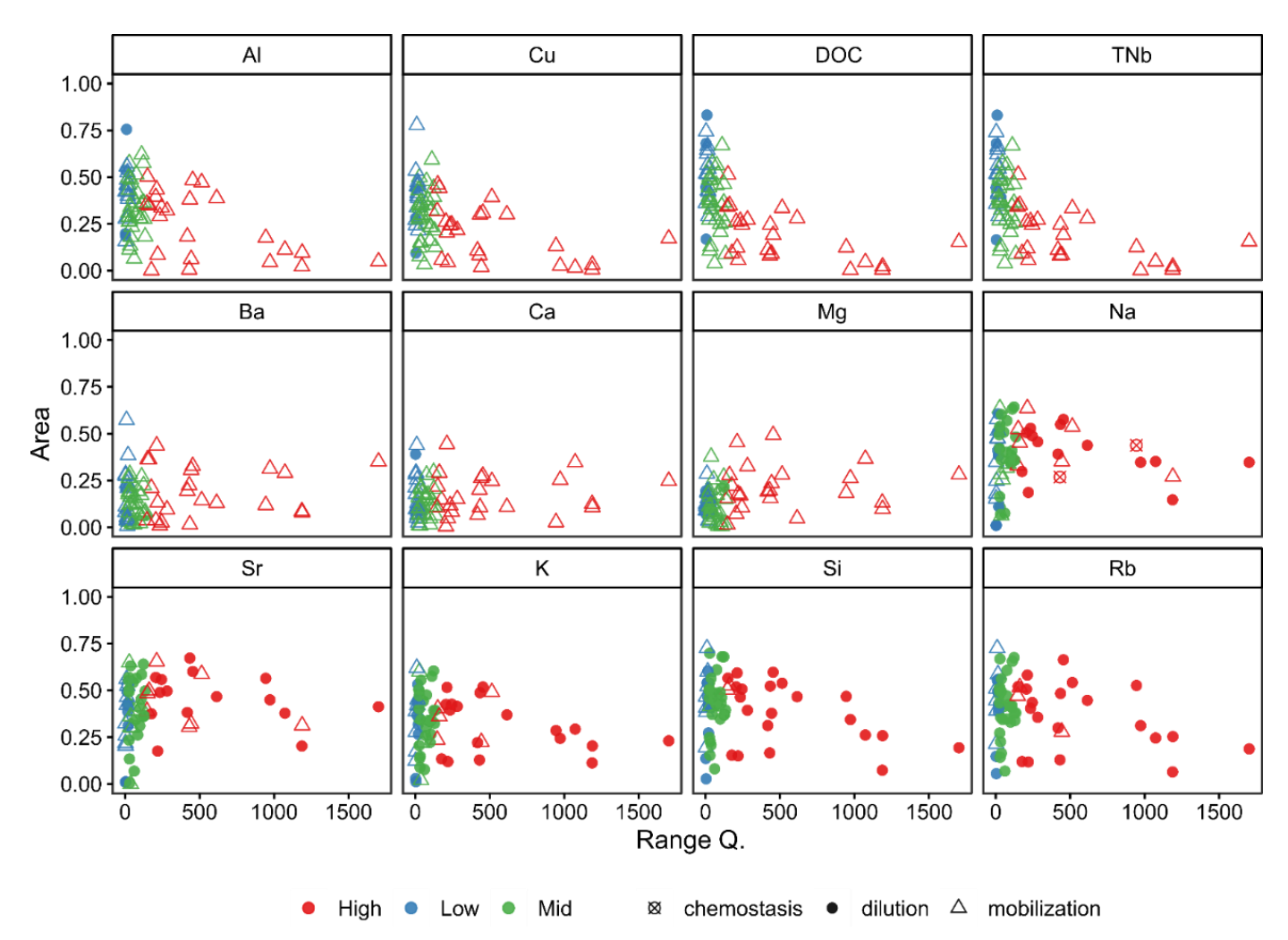


**Figure 6** Visual relationships between range of discharge (Range Q.) and the hysteresis loop area for each element. A dot represents a single hydrological event and it is categorized according to its chemical state (shape: chemostasis, dilution, mobilization) and its flow rate (color: high, mid, low). The solutes are ordered according to anti-clockwise domain, mixed and clockwise domain classification, respectively.

From *Figure 6*, we can conclude that growing values of range Q (high-flow rates) produces a tendency of loop area to 0. It denotes that the loop shape inclines to a low-area figure 8 or a direct hysteresis response. Nevertheless, mixed group seems not to share this tendency, the dot distribution remains constant. To low-flow and mid-flow rates, there is no clear relationship between range of discharge and loop area, it is highly variable.



Anti-clockwise domain and mixed groups indicate dilution chemical states at low-flow discharge rates but there are a few events that point out mobilization performance. Midflow and high-flow discharge rates correspond to mobilization chemical states. Conversely, clockwise domain solutes have an opposite manner: mobilization at low-flow rates and dilution at mid-flow and high-flow. Still, we can find a small number of events that display mobilization chemical states at mid-flow and high-flow discharge rates, or dilution at low-flow rates.

#### 4. Discussion

#### 4.1 Hysteresis Loop Characterization

The results indicate the presence of our denominated domain groups (anti-clockwise, clockwise, mixed) with their characteristically solutes: Al, Cu, DOC and TNb for the anticlockwise; Na, Sr, K, Si and Rb for the clockwise domain group; Ba, Ca and Mg for the mixed group (Figure 2). It has been suggested that anti-clockwise hysteresis responses indicate distant locations between the solute source and the monitoring point (de Barros et al., 2020; Mao & Carrillo, 2017; Misset et al., 2019; Rodríguez-Blanco et al., 2018). However, we assume that there are two key points causing anti-clockwise C-Q relationships in our studied system. The first key point corresponds to the seasonal variability of rainfall and runoff distribution, as well as the solute production in the catchment. Under low-flow conditions, lowest soil sources of solutes (spring water) represent one of the most important contributors to stream chemistry. Conversely, at highflow stages, shallow soil sources (Histosols) take over the contribution to stream chemistry (Correa et al., 2017). Then, the transition from low-flow to high-flow conditions causes a quicker growth of concentration values than discharge values of solutes with strong presence at Histosols (Al, Cu, DOC and TNb), producing the anti-clockwise characteristically delay between concentration peak and discharge peak during the hydrological event. This also accords with earlier observations (Shi et al., 1985; Williams, 1989), which showed similar lagged interaction between concentration and discharge due

to the annual rise and fall of water and solute concentrations at downstream sites during storm events. The second key point is the superficial location of solute sources (Histosols). Storm events generate continuous AI, Cu, DOC and TNb pulses in the stream chemical signature due to high contents of organometallic compounds (organic matter + AI, Fe) in Histosols (Castañeda-Martín & Montes-Pulido, 2017; Mosquera et al., 2015; Pesántez et al., 2018; Quichimbo, 2012). This characteristic drives to an anti-clockwise hysteresis response, given that concentration growth rates are faster than discharge ones (Williams, 1989).

Mainly, clockwise hysteresis responses have been associated with short distances between the solute source and the monitoring point (Long et al., 2017; Mao & Carrillo, 2017; Peraza-Castro et al., 2016). Nevertheless, we consider a more significant cause of clockwise C-Q relationships, which is the small supply at solute sources and their deep soil location in the catchment, activated during dry seasons by underground water contributions to the stream. Solutes that belong to the clockwise domain group, such as Na, Sr, K, Si, and Rb, have the strongest presence at deep soil locations (Correa et al., 2017, 2019), pointing them out as the mainly solute source. After a dry period, the first rainfalls infiltrate quickly producing a water table rising which will contribute to the stream easily (Correa et al., 2019). This underground solute origin has been reported by several prior studies (Arnborg et al., 1967; VanSickle & Beschta, 1983; Walling & E., 1974; Williams, 1989; Wood, 1977), which identified underground solute sources as the main driver of early depletion of concentration when discharge reaches its peak during the event.

Figure 2 shows the constantly presence of figure 8 hysteresis responses (at least 20 %) to each analyzed solute. Solutes from both clockwise (Na, Sr, K, Si and Rb) and mixed (Ba, Ca and Mg) domain groups have their main contribution source at underground locations (Correa et al., 2017), hinting a production of clockwise hysteresis responses at early stages of dry seasons. After a clockwise loop, flow rates grow and catchment facilitates solute transportation, producing a slower concentration decay in comparison to discharge. This interaction, at the falling limb of the hydrograph, generates an anti-

clockwise loop. In conjunction, a clockwise loop followed by an anti-clockwise loop generate a figure 8 hysteresis loop. On the other hand, solutes from the anti-clockwise domain group (Al, Cu, DOC and TNb) show an inverse figure 8 hysteresis dynamic: after an anti-clockwise loop, high flow rates drive to a solute depletion in the stream, producing a faster concentration decay in comparison to discharge (clockwise loop). Comparison of this findings with the study performed by Williams (1989) confirms similar figure 8 hysteresis responses, all attributed to the latter mentioned interaction.

Direct hysteresis responses are detected on solutes with deep ground origins (*Figure 2*), especially the solutes from the mixed domain group which exhibit a notorious presence of direct events (12 % - 17 %). These atypical hysteresis C-Q relationships are related to extremely high flow rates, so they can trigger a continuous solute supply during the event, especially at wet antecedent conditions when the hydrologic response is very fast. This uninterrupted supply drives to a synchronized decrease of concentration and discharge magnitudes which leads to direct hysteresis responses. This also accords with earlier observations (Williams, 1989; Wood, 1977).

#### 4.2 Analysis of the Hysteresis Indicators Variability Controls

The evolution of the chemical status along the studied period (*Figure 4*), points out marked behaviors for solutes that belong to the anti-clockwise (DOC) and mixed (Ca) dominance groups (*Figure 4*, *a* and *c*). Interestingly, HI and loop area values decrease as the magnitude of the event increases, reinforcing the idea that solutes tend to trigger figure 8 hysteresis responses (HI  $\approx$  0) as flow rates increase. This not appear to be the case in Na, given that the hysteresis indicators value remains similar as the magnitude of the events increase or decrease (*Figure 4b*).

Our results stated that discharge represents the most important factor on anti-clockwise hysteresis responses. As discharge rates increase, storm events activate the solute concentration increase at stream, highlighting shallow solute sources to the stream. Prior



studies developed in the study zone indicate high contents of organometallic compounds in the chemical signature of Histosols, corresponding to the mentioned shallow solute sources (Castañeda-Martín & Montes-Pulido, 2017; Correa et al., 2017, 2019; Mosquera et al., 2015; Quichimbo, 2012). This high solute content in Histosols leads to a steady state of solute production, evidenced in the influence of concentration variables in HI (DOC and TNb, Table 2) and the clear tendency to mobilization chemical status during mid-flow and high-flow rates (Figure 5, Figure 6). This statement agrees with Correa et al. (2017), that establish Andosols and Histosols as the main contributors to runoff in its generation process and Moatar et al. (2017); Wymore et al. (2017) that evidenced mobilization behaviors for DOC on their study watersheds, resulting in an increasing DOC concentration values as discharge rates grow. In reviewing the literature, very little was found on the association between hydrological control factors and anti-clockwise hysteresis behavior. Nevertheless, Lloyd et al. (2016a); Rodríguez-Blanco et al. (2018) share analogous outcomes in terms of identifying anti-clockwise controls. They set discharge variables and antecedent rainfall conditions as triggering factors of this particular hysteresis response.

An overview of our results divides the main drivers for clockwise hysteresis into two stages, the first one establishes that the HI and loop area variability of Na, Sr, and K depends on discharge and concentration rates (*Table 3*, *Table 4*). The relative high r values of concentration denote the influence of the solute availability in its depletion caused by an increase of discharge rates (dilution chemical state *Figure 5*, *Figure 6*), similar dilution patterns were exposed by Stallard & Murphy (2013) and Wymore et al. (2017) on solutes originated from bedrock weathering processes (Si and Mg) on watersheds with volcaniclastic lithology. The second stage implies an exclusive influence of discharge variables. Negative r values of discharge variables (Si and Rb *Table 3*, *Table 4*) suggest a relative high probability to find clockwise responses at low-flow conditions. What is interesting in these solutes, is the moderate impact of the duration event, their negative r values insinuate a better development of clockwise hysteresis during short

events. We can say now that clockwise hysteresis behaviors are more likely to occur in short-duration events with low-flow rates after dry periods. Similar conclusions are reported by (Bieroza & Heathwaite, 2015; Knapp et al., 2020; Tardy et al., 2004), particularly the main controls on clockwise hysteresis response and its consequential interactions between groundwater and surface water.

Discharge rates represent important controls of figure 8 and direct hysteresis responses. As we mentioned before, high-flow conditions make the catchment generate a steady state of solute supply, driving to these types of hysteresis loops. These relationships may partly be explained by the HI tendency to zero, as discharge increases (*Figure 5*, *Figure 6*). Also, the fact that discharge variables have higher r values than precipitation and concentration variables (*Table 3*), helps us to corroborate the previous statement about discharge being a key control factor on figure 8 and direct responses. These results reflect those of Stallard & Murphy (2013) who also found that runoff generation processes are more linked to the solute chemical status than geology, soils and land cover. Dilution of non-bioactive solutes (Ca, Mg, Na) is related to bedrock weathering and atmospheric deposition. Mobilization, on the other hand, is usually associated to shallow soil sources of bioactive solutes (i.e.: DOC) (Godsey et al., 2019; Stallard & Murphy, 2013). This is evidenced in the tendency to dilution and mobilization chemical states from solutes with deep ground origins and solutes with shallow origins, respectively (*Figure 5*, *Figure 6*).

Several prior studies have been suggested that the variability in hysteresis responses among different hydrologic events and solutes are linked to antecedent rainfall conditions (Bieroza & Heathwaite, 2015; Knapp et al., 2020). This does not appear to be the case, excepting for particular instances such as Ba and Ca solutes. Their loop area is influenced by antecedent precipitation variables (Mean 72, Mean 96 and Mean 120 *Table 3*). We attributed this precipitation influence to atmospheric solute deposition and resuspension processes of solutes accumulated on the stream bed, during low-flow seasons (D. J. Evans et al., 2004; Stallard & Murphy, 2013).



#### 5. Conclusions

The purpose of the current study was to determine the main hydrometeorological controls of hysteresis metrics variability, considering a wide range of solutes (Al, Cu, DOC, TNb, Ba, Ca, Mg, Na, Sr, K, Si, Rb) in a small high-mountain tropical catchment. The results of this investigation show that solutes can be classified into three different groups according to their principal hysteresis response, these are anti-clockwise dominance (Al, Cu, DOC and TNb), clockwise dominance (Na, Sr, K, Si and Rb) and the last one has mixed presences of the four hysteresis types (Ba, Ca and Mg). Both correlation and random forest analysis revealed that discharge represents the most influencing variable on the hysteresis response. For HI, specifically, range of discharge exhibits the biggest impact, pointing a close relationship between flow rates and hysteresis loop quantifications. However, the effects of discharge variables on loop area are less dominant. Here we can find punctual cases like Ba which is influenced directly by antecedent precipitation rates (mean 72, mean 96 and mean 120). Overall, this study strengthens the idea that solutes originated from weathering bedrock processes at deep ground locations (Na, Sr, K, Si, and Rb), tend to exhibit clockwise hysteresis responses and therefore dilution patterns of solute concentrations as flow rates increase. On the other hand, solutes originated at shallow locations (Al, Cu, DOC and TNb) such as Histosols, display anti-clockwise hysteresis behaviors. Thus, mobilization patterns of solute concentrations are evidenced as flow rates increase. The findings of this study contribute to our understanding of the hydrometeorological processes that govern the varied stream chemistry response in a small high-mountain tropical catchment.

#### 6. References

Arnborg, L., Walker, H. J., & Peippo, J. (1967). Suspended Load in the Colville River, Alaska, 1962. *Geografiska Annaler: Series A, Physical Geography*, 49(2–4), 131–144. https://doi.org/10.1080/04353676.1967.11879744

- Basu, N. B., Destouni, G., Jawitz, J. W., Thompson, S. E., Loukinova, N. v., Darracq, A., Zanardo, S., Yaeger, M., Sivapalan, M., Rinaldo, A., & Rao, P. S. C. (2010). Nutrient loads exported from managed catchments reveal emergent biogeochemical stationarity. *Geophysical Research Letters*, 37(23). https://doi.org/10.1029/2010GL045168
- Basu, N. B., Thompson, S. E., & Rao, P. S. C. (2011). Hydrologic and biogeochemical functioning of intensively managed catchments: A synthesis of top-down analyses. *Water Resources Research*, *47*(10). https://doi.org/10.1029/2011WR010800
- Bieroza, M. Z., & Heathwaite, A. L. (2015). Seasonal variation in phosphorus concentration-discharge hysteresis inferred from high-frequency in situ monitoring. *Journal of Hydrology*, *524*, 333–347. https://doi.org/10.1016/j.jhydrol.2015.02.036
- Biron, P. M., Roy, A. G., Courschesne, F., Hendershot, W. H., Côté, B., & Fyles, J. (1999). The effects of antecedent moisture conditions on the relationship of hydrology to hydrochemistry in a small forested watershed. *Hydrological Processes*, 13(11), 1541–1555. https://doi.org/10.1002/(SICI)1099-1085(19990815)13:11<1541::AID-HYP832>3.0.CO;2-J
- Bowes, M. J., Jarvie, H. P., Halliday, S. J., Skeffington, R. A., Wade, A. J., Loewenthal, M., Gozzard, E., Newman, J. R., & Palmer-Felgate, E. J. (2015). Characterising phosphorus and nitrate inputs to a rural river using high-frequency concentration-flow relationships. *Science of the Total Environment*, *511*, 608–620. https://doi.org/10.1016/j.scitotenv.2014.12.086
- Bowes, M. J., Smith, J. T., & Neal, C. (2009). The value of high-resolution nutrient monitoring: A case study of the River Frome, Dorset, UK. *Journal of Hydrology*, 378(1–2), 82–96. https://doi.org/10.1016/j.jhydrol.2009.09.015
- Breiman, L., Friedman, J., Stone, C. J., & Olshen, R. A. (1984). *Classification and regression trees*.
- Butturini, A., Alvarez, M., Bernał, S., Vazquez, E., & Sabater, F. (2008). Diversity and temporal sequences of forms of DOC and NO3- discharge responses in an intermittent stream: Predictable or random succession? *Journal of Geophysical Research: Biogeosciences*, 113(3). https://doi.org/10.1029/2008JG000721
- Buytaert, W., & Beven, K. (2011). Models as multiple working hypotheses: Hydrological simulation of tropical alpine wetlands. *Hydrological Processes*, *25*(11), 1784–1799. https://doi.org/10.1002/hyp.7936

- Buytaert, W., Deckers, J., & Wyseure, G. (2006). Description and classification of nonallophanic Andosols in south Ecuadorian alpine grasslands (páramo). Geomorphology, 73(3–4), 207–221. https://doi.org/10.1016/j.geomorph.2005.06.012
- Castañeda-Martín, A. E., & Montes-Pulido, C. R. (2017). Carbono almacenado en páramo andino. *ENTRAMADO*, *13*(1), 210–221. https://doi.org/10.18041/entramado.2017v13n1.25112
- Chanat, J. G., Rice, K. C., & Hornberger, G. M. (2002). Consistency of patterns in concentration-discharge plots. *Water Resources Research*, *38*(8), 22-1-22–10. https://doi.org/10.1029/2001wr000971
- Clow, D. W., & Mast, M. A. (2010). Mechanisms for chemostatic behavior in catchments: Implications for CO 2 consumption by mineral weathering. *Chemical Geology*, 269(1–2), 40–51. https://doi.org/10.1016/j.chemgeo.2009.09.014
- Coltorti, M., & Ollier, C. D. (2000). Geomorphic and tectonic evolution of the Ecuadorian Andes. *Geomorphology*, 32(1–2), 1–19. https://doi.org/10.1016/S0169-555X(99)00036-7
- Correa, A., Breuer, L., Crespo, P., Célleri, R., Feyen, J., Birkel, C., Silva, C., & Windhorst, D. (2019). Spatially distributed hydro-chemical data with temporally high-resolution is needed to adequately assess the hydrological functioning of headwater catchments. *Science of the Total Environment*, *651*, 1613–1626. https://doi.org/10.1016/j.scitotenv.2018.09.189
- Correa, A., Windhorst, D., Tetzlaff, D., Crespo, P., Célleri, R., Feyen, J., & Breuer, L. (2017). Temporal dynamics in dominant runoff sources and flow paths in the Andean Páramo. *Water Resources Research*, *53*(7), 5998–6017. https://doi.org/10.1002/2016WR020187
- Creed, I. F., McKnight, D. M., Pellerin, B. A., Green, M. B., Bergamaschi, B. A., Aiken, G. R., Burns, D. A., Findlay, S. E. G., Shanley, J. B., Striegl, R. G., Aulenbach, B. T., Clow, D. W., Laudon, H., McGlynn, B. L., McGuire, K. J., Smith, R. A., & Stackpoole, S. M. (2015). The river as a chemostat: fresh perspectives on dissolved organic matter flowing down the river continuum. *Canadian Journal of Fisheries and Aquatic Sciences*, 72(8), 1272–1285. https://doi.org/10.1139/cjfas-2014-0400
- Crespo, P. J., Feyen, J., Buytaert, W., Bücker, A., Breuer, L., Frede, H. G., & Ramírez, M. (2011). Identifying controls of the rainfall-runoff response of small catchments in

- the tropical Andes (Ecuador). *Journal of Hydrology*, *407*(1–4), 164–174. https://doi.org/10.1016/j.jhydrol.2011.07.021
- Daley, M. L., Potter, J. D., & McDowell, W. H. (2009). Salinization of urbanizing New Hampshire streams and groundwater: Effects of road salt and hydrologic variability. *Journal of the North American Benthological Society*, 28(4), 929–940. https://doi.org/10.1899/09-052.1
- de Barros, C. A. P., Tiecher, T., Ramon, R., dos Santos, D. R., Bender, M. A., Evrard, O., Ayrault, S., & Minella, J. P. G. (2020). Investigating the relationships between chemical element concentrations and discharge to improve our understanding of their transport patterns in rural catchments under subtropical climate conditions. *Science of The Total Environment*, 141345. https://doi.org/10.1016/j.scitotenv.2020.141345
- Evans, C., & Davies, T. D. (1998). Causes of concentration/discharge hysteresis and its potential as a tool for analysis of episode hydrochemistry. *Water Resources Research*, *34*(1), 129–137. https://doi.org/10.1029/97WR01881
- Evans, D. J., Johnes, P. J., & Lawrence, D. S. (2004). Physico-chemical controls on phosphorus cycling in two lowland streams. Part 2-The sediment phase. *Science of the Total Environment*, 329(1–3), 165–182. https://doi.org/10.1016/j.scitotenv.2004.02.023
- Godsey, S. E., Hartmann, J., & Kirchner, J. W. (2019). Catchment chemostasis revisited: Water quality responds differently to variations in weather and climate. *Hydrological Processes*, *33*(24), 3056–3069. https://doi.org/10.1002/hyp.13554
- Godsey, S. E., Kirchner, J. W., & Clow, D. W. (2009). Concentration-discharge relationships reflect chemostatic characteristics of US catchments. *Hydrological Processes*, *23*(13), 1844–1864. https://doi.org/10.1002/hyp.7315
- Hale, R. L., & Godsey, S. E. (2019). Dynamic stream network intermittence explains emergent dissolved organic carbon chemostasis in headwaters. *Hydrological Processes*, 33(13), 1926–1936. https://doi.org/10.1002/HYP.13455
- Heidel, S. G. (1956). The progressive lag of sediment concentration with flood waves. *Eos, Transactions American Geophysical Union*, *37*(1), 56–66. https://doi.org/10.1029/TR037i001p00056

- Herndon, E. M., Dere, A. L., Sullivan, P. L., Norris, D., Reynolds, B., & Brantley, S. L. (2015). Landscape heterogeneity drives contrasting concentration-discharge relationships in shale headwater catchments. *Hydrology and Earth System Sciences*, 19(8), 3333–3347. https://doi.org/10.5194/hess-19-3333-2015
- Hornberger, G. M., Scanlon, T. M., & Raffensperger, J. P. (2001). Modelling transport of dissolved silica in a forested headwater catchment: the effect of hydrological and chemical time scales on hysteresis in the concentration-discharge relationship. *Hydrological Processes*, *15*(10), 2029–2038. https://doi.org/10.1002/hyp.254
- Hungerbühler, D., Steinmann, M., Winkler, W., Seward, D., Egüez, A., Peterson, D. E., Helg, U., & Hammer, C. (2002). Neogene stratigraphy and Andean geodynamics of southern Ecuador. *Earth-Science Reviews*, *57*(1–2), 75–124. https://doi.org/10.1016/S0012-8252(01)00071-X
- Ibarra, D. E., Caves, J. K., Moon, S., Thomas, D. L., Hartmann, J., Chamberlain, C. P., & Maher, K. (2016). Differential weathering of basaltic and granitic catchments from concentration—discharge relationships. *Geochimica et Cosmochimica Acta*, 190, 265–293. https://doi.org/10.1016/j.gca.2016.07.006
- Jiang, R., Woli, K. P., Kuramochi, K., Hayakawa, A., Shimizu, M., & Hatano, R. (2010). Hydrological process controls on nitrogen export during storm events in an agricultural watershed. Soil Science and Plant Nutrition, 56(1), 72–85. https://doi.org/10.1111/j.1747-0765.2010.00456.x
- Jones, A. S., Stevens, D. K., Horsburgh, J. S., & Mesner, N. O. (2011). Surrogate Measures for Providing High Frequency Estimates of Total Suspended Solids and Total Phosphorus Concentrations1. *JAWRA Journal of the American Water Resources Association*, 47(2), 239–253. https://doi.org/10.1111/j.1752-1688.2010.00505.x
- Kirchner, J. W., Feng, X., Neal, C., & Robson, A. J. (2004). The fine structure of water-quality dynamics: The (high-frequency) wave of the future. *Hydrological Processes*, *18*(7), 1353–1359. https://doi.org/10.1002/hyp.5537
- Knapp, J., von Freyberg, J., Studer, B., Kiewiet, L., & Kirchner, J. (2020). Concentration-discharge relationships vary among hydrological events, reflecting differences in event characteristics. *Hydrology and Earth System Sciences Discussions*, 1–27. https://doi.org/10.5194/hess-2019-684

- Langlois, J. L., Johnson, D. W., & Mehuys, G. R. (2005). Suspended sediment dynamics associated with snowmelt runoff in a small mountain stream of Lake Tahoe (Nevada). *Hydrological Processes*, *19*(18), 3569–3580. https://doi.org/10.1002/hyp.5844
- Lang, M., Ouarda, T. B. M. J., & Bobée, B. (1999). Towards operational guidelines for over-threshold modeling. In *Journal of Hydrology* (Vol. 225, Issues 3–4, pp. 103– 117). Elsevier. https://doi.org/10.1016/S0022-1694(99)00167-5
- Lawler, D. M., Petts, G. E., Foster, I. D. L., & Harper, S. (2006). Turbidity dynamics during spring storm events in an urban headwater river system: The Upper Tame, West Midlands, UK. *Science of the Total Environment*, *360*(1–3), 109–126. https://doi.org/10.1016/j.scitotenv.2005.08.032
- Liaw, A., & Wiener, M. (2002). *Classification and Regression by RandomForest*. https://www.researchgate.net/publication/228451484
- Lloyd, C. E. M., Freer, J. E., Johnes, P. J., & Collins, A. L. (2016a). Using hysteresis analysis of high-resolution water quality monitoring data, including uncertainty, to infer controls on nutrient and sediment transfer in catchments. *Science of the Total Environment*, *543*, 388–404. https://doi.org/10.1016/j.scitotenv.2015.11.028
- Lloyd, C. E. M., Freer, J. E., Johnes, P. J., & Collins, A. L. (2016b). Technical Note: Testing an improved index for analysing storm discharge-concentration hysteresis. *Hydrology and Earth System Sciences*, 20(2), 625–632. https://doi.org/10.5194/hess-20-625-2016
- Long, D. T., Voice, T. C., Xagaroraki, I., Chen, A., Wu, H., Lee, E., Oun, A., & Xing, F. (2017). Patterns of c-q hysteresis loops and within an integrative pollutograph for selected inorganic and organic solutes and E. coli in an urban salted watershed during winter-early spring periods. *Applied Geochemistry*, 83, 93–107. https://doi.org/10.1016/j.apgeochem.2017.03.002
- Madrid, Y., & Zayas, Z. P. (2007). Water sampling: Traditional methods and new approaches in water sampling strategy. *TrAC Trends in Analytical Chemistry*, 26(4), 293–299. https://doi.org/10.1016/j.trac.2007.01.002
- Maher, K. (2011). The role of fluid residence time and topographic scales in determining chemical fluxes from landscapes. *Earth and Planetary Science Letters*, 312(1–2), 48–58. https://doi.org/10.1016/j.epsl.2011.09.040

- Mao, L., & Carrillo, R. (2017). Temporal dynamics of suspended sediment transport in a glacierized Andean basin. *Geomorphology*, *287*, 116–125. https://doi.org/10.1016/j.geomorph.2016.02.003
- McClain, M. E., Boyer, E. W., Dent, C. L., Gergel, S. E., Grimm, N. B., Groffman, P. M., Hart, S. C., Harvey, J. W., Johnston, C. A., Mayorga, E., McDowell, W. H., & Pinay, G. (2003). Biogeochemical Hot Spots and Hot Moments at the Interface of Terrestrial and Aquatic Ecosystems on JSTOR. *Ecosystems*, *6*. https://www.jstor.org/stable/3659030?seg=1
- Misset, C., Recking, A., Legout, C., Poirel, A., Cazilhac, M., Esteves, M., & Bertrand, M. (2019). An attempt to link suspended load hysteresis patterns and sediment sources configuration in alpine catchments. *Journal of Hydrology*, *576*, 72–84. https://doi.org/10.1016/j.jhydrol.2019.06.039
- Moatar, F., Abbott, B. W., Minaudo, C., Curie, F., & Pinay, G. (2017). Elemental properties, hydrology, and biology interact to shape concentration-discharge curves for carbon, nutrients, sediment, and major ions. *Water Resources Research*, *53*(2), 1270–1287. https://doi.org/10.1002/2016WR019635
- Moore, R. D. (2004). Introduction to Salt Dilution Gauging for Streamflow Measurement Part 2: Constant-rate Injection. *Streamline Watershed Management Bulletin*, 8, 11–15.
- Mosquera, G. M., Lazo, P. X., Célleri, R., Wilcox, B. P., & Crespo, P. (2015). Runoff from tropical alpine grasslands increases with areal extent of wetlands. *Catena*, 125, 120–128. https://doi.org/10.1016/j.catena.2014.10.010
- Murphy, J. C., Hornberger, G. M., & Liddle, R. G. (2014). Concentration-discharge relationships in the coal mined region of the New River basin and Indian Fork subbasin, Tennessee, USA. *Hydrological Processes*, *28*(3), 718–728. https://doi.org/10.1002/hyp.9603
- O'Kane, J. (2005). Hysteresis in hydrology. *Acta Geophysica Polonica*, *53*, 373–383. https://www.infona.pl/resource/bwmeta1.element.baztech-article-BSL7-0009-0040
- Padrón, R. S., Wilcox, B. P., Crespo, P., & Célleri, R. (2015). Rainfall in the andean páramo: New insights from high-resolution monitoring in southern Ecuador. *Journal of Hydrometeorology*, *16*(3), 985–996. https://doi.org/10.1175/JHM-D-14-0135.1

- Peraza-Castro, M., Sauvage, S., Sánchez-Pérez, J. M., & Ruiz-Romera, E. (2016). Effect of flood events on transport of suspended sediments, organic matter and particulate metals in a forest watershed in the Basque Country (Northern Spain). Science of the Total Environment, 569–570, 784–797. https://doi.org/10.1016/j.scitotenv.2016.06.203
- Pesántez, J., Birkel, C., Mosquera, G. M., Peña, P., Arízaga-Idrovo, V., Mora, E., McDowell, W. H., & Crespo, P. (2021). High-frequency multi-solute calibration using an in situ UV–visible sensor. *Hydrological Processes*, *35*(9), e14357. https://doi.org/10.1002/HYP.14357
- Pesántez, J., Mosquera, G. M., Crespo, P., Breuer, L., & Windhorst, D. (2018). Effect of land cover and hydro-meteorological controls on soil water DOC concentrations in a high-elevation tropical environment. *Hydrological Processes*, *32*(17), 2624–2635. https://doi.org/10.1002/hyp.13224
- Phillips, J. D. (2003). Sources of nonlinearity and complexity in geomorphic systems. *Progress in Physical Geography*, *27*(1), 1–23. https://doi.org/10.1191/0309133303pp340ra
- Pratt, W. T., Figueroa, J. F., & Flores, B. G. (1997). Geology of the Cordillera Occidental of Ecuador between 3 00'and 4 00'S. *World Bank Mining Development*.
- Quichimbo, P. (2012). Efectos sobre las propiedades físicas y químicas de los suelos por el cambio de la cobertura vegetal y uso del suelo: Páramo de Quimsacocha al sur del Ecuador. In *researchgate.net*. https://www.researchgate.net/publication/285632863
- Ramsay, P. M., & Oxley, E. R. B. (1997). The growth form composition of plant communities in the Ecuadorian paramos. *Plant Ecology*, *131*(2), 173–192. https://doi.org/10.1023/A:1009796224479
- Ribatet, M., & Dutang, C. (2018). *POT: Generalized Pareto Distribution and Peaks Over Threshold* (version 1.1-7.). R package.
- Robson, A., Jenkins, A., & Neal, C. (1991). Towards predicting future episodic changes in stream chemistry. *Journal of Hydrology*, *125*(3–4), 161–174. https://doi.org/10.1016/0022-1694(91)90027-F
- Rodríguez-Blanco, M. L., Soto-Varela, F., Taboada-Castro, M. M., & Taboada-Castro, M. T. (2018). Using hysteresis analysis to infer controls on sediment-associated and

- dissolved metals transport in a small humid temperate catchment. *Journal of Hydrology*, *565*, 49–60. https://doi.org/10.1016/j.jhydrol.2018.08.030
- Seeger, M., Errea, M. P., Beguería, S., Arnáez, J., Martí, C., & García-Ruiz, J. M. (2004). Catchment soil moisture and rainfall characteristics as determinant factors for discharge/suspended sediment hysteretic loops in a small headwater catchment in the Spanish pyrenees. *Journal of Hydrology*, 288(3–4), 299–311. https://doi.org/10.1016/j.jhydrol.2003.10.012
- Shanley, J. B., Sebestyen, S. D., Mcdonnell, J. J., Mcglynn, B. L., & Dunne, T. (2015). Water's Way at Sleepers River watershed revisiting flow generation in a post-glacial landscape, Vermont USA. *Hydrological Processes*, *29*(16), 3447–3459. https://doi.org/10.1002/hyp.10377
- Shi, Y.-L., Yang, W., & Ren, M.-E. (1985). Hydrological characteristics of the Changjiang and its relation to sediment transport to the sea. *Continental Shelf Research*, *4*(1–2), 5–15. https://doi.org/10.1016/0278-4343(85)90018-4
- Sklenar, P., & Jorgensen, P. M. (1999). Distribution patterns of paramo plants in Ecuador. *Journal of Biogeography*, *26*(4), 681–691. https://doi.org/10.1046/j.1365-2699.1999.00324.x
- Spence, C. (2010). A paradigm shift in hydrology: Storage thresholds across scales influence catchment Runoff Generation. In *Geography Compass* (Vol. 4, Issue 7, pp. 819–833). John Wiley & Sons, Ltd. https://doi.org/10.1111/j.1749-8198.2010.00341.x
- Stallard, R. F., & Murphy, S. F. (2013). A Unified Assessment of Hydrologic and Biogeochemical Responses in Research Watersheds in Eastern Puerto Rico Using Runoff–Concentration Relations. *Aquatic Geochemistry 2013 20:2*, *20*(2), 115–139. https://doi.org/10.1007/S10498-013-9216-5
- Tardy, Y., Bustillo, V., & Boeglin, J. L. (2004). Geochemistry applied to the watershed survey: hydrograph separation, erosion and soil dynamics. A case study: the basin of the Niger River, Africa. *Applied Geochemistry*, *19*(4), 469–518. https://doi.org/10.1016/J.APGEOCHEM.2003.07.003
- Therneau, T., & Atkinson, B. (2019). *rpart: Recursive Partitioning and Regression Trees* (R package version 4.1-15). https://CRAN.R-project.org/package=rpart

- U.S. Bureau of Reclamation. (2001). Water Measurement Manual. Washington DC. USDA, NRCS, 2004. Soil Survey Laboratory Methods Manual: Soil Survey Investigations Report No. 42, Version 4.0, November 2004.
- VanSickle, J., & Beschta, R. L. (1983). Supply-based models of suspended sediment transport in streams. *Water Resources Research*, *19*(3), 768–778. https://doi.org/10.1029/WR019i003p00768
- Walling, & E., D. (1974). Suspended sediment and solid yields from a small catchment prior to urbanization. *Fluvial Processes in Instrumented Watersheds*, *6*, 169–192. https://ci.nii.ac.jp/naid/10007536169
- Williams, G. P. (1989). SEDIMENT CONCENTRATION VERSUS WATER DISCHARGE DURING SINGLE HYDROLOGIC EVENTS IN RIVERS. In *Journal of Hydrology* (Vol. 111).
- Winnick, M. J., Carroll, R. W. H., Williams, K. H., Maxwell, R. M., Dong, W., & Maher, K. (2017). Snowmelt controls on concentration-discharge relationships and the balance of oxidative and acid-base weathering fluxes in an alpine catchment, East River, Colorado. Water Resources Research, 53(3), 2507–2523. https://doi.org/10.1002/2016WR019724
- Wood, P. A. (1977). Controls of variation in suspended sediment concentration in the River Rother, West Sussex, England. *Sedimentology*, *24*(3), 437–445. https://doi.org/10.1111/j.1365-3091.1977.tb00131.x
- Wymore, A. S., Brereton, R. L., Ibarra, D. E., Maher, K., & McDowell, W. H. (2017). Critical zone structure controls concentration-discharge relationships and solute generation in forested tropical montane watersheds. *Water Resources Research*, 53(7), 6279–6295. https://doi.org/10.1002/2016WR020016
- Zuecco, G., Penna, D., Borga, M., & van Meerveld, H. J. (2016). A versatile index to characterize hysteresis between hydrological variables at the runoff event timescale. *Hydrological Processes*, *30*(9), 1449–1466. https://doi.org/10.1002/hyp.10681